Journal of
Applied Crystallography
ISSN 0021-8898

Received 27 March 2000
Accepted 31 May 2000

A novel free-mounting system for protein crystals: transformation and improvement of diffraction power by accurately controlled humidity changes

Reiner Kiefersauer,[a,b]* Manuel E. Than,[a] Holger Dobbek,[a] Lothar Gremer,[c] Marcos Melero,[a] Stefan Strobl,[a] João M. Dias,[a,d] Tewfik Soulimane[e] and Robert Huber[a]

[a]Max-Planck-Institut für Biochemie, am Klopferspitz 18a, D-82152 Martinsried, Germany, [b]Proteros, am Klopferspitz 19, D-82152 Martinsried, Germany, [c]Lehrstuhl für Mikrobiologie, Universität Bayreuth, D-95440 Bayreuth, Germany, [d]Departamento de Quimica, CQFB, FCT, Universidade Nova de Lisboa, 2825-114 Caparica, Portugal, and [e]Rheinisch-Westfälische Technische Hochschule Aachen, Institut für Biochemie, Pauwelsstr. 30, D-52057 Aachen, Germany. Correspondence e-mail: kiefersa@biochem.mpg.de

A novel device for capillary-free mounting of protein crystals is described. A controlled stream of air allows an accurate adjustment of the humidity at the crystal. The crystal is held on the tip of a micropipette. With a video system (CCD camera), the two-dimensional shadow projections of crystals can be recorded for optical analysis. Instead of the micropipette, a standard loop can also be used. Experiments and results for different crystal systems demonstrate the use of this method, also in combination with shock-freezing, to improve crystal order. Working with oxygen-free gases offers the possibility of crystal measurements under anaerobic conditions. Furthermore, the controlled application of arbitrary volatile substances with the gas stream is practicable.

1. Introduction

The success of protein crystallography in recent years rests on the development of methods and techniques in molecular biology, recombinant protein expression, protein chemistry and on the accessibility of high-intensity and tunable X-ray sources, X-ray detectors, cryo-techniques and computing power. On the other hand, the crystallization of protein crystals of sufficient quality is still a game of trial and error.

The large size and the irregular shape of the protein molecules and the absence of strong intermolecular forces are reasons that protein crystals are held together rather weakly. They have high solvent contents, around 30 to 70% or even as much as 90% (McPherson *et al.*, 1995). Consequently, protein crystals are often unstable and poorly ordered.

One approach to obtain suitable crystals is to manipulate the already grown crystals. The first systematic experiments in that direction were performed by Perutz and Kendrew (Bragg & Perutz, 1952; Huxley & Kendrew, 1953). They mounted crystals in glass capillaries connected to a salt reservoir. Varying the relative humidity (r.h.) in the capillary by changing the salt concentration produced different crystal forms. A similar experiment can be performed with crystals in mother liquor by changing the concentration of the storage buffer. The first example was the EF-Tu·EF-Ts complex (Schick & Jurnak, 1994). By accident, it was found that by increasing the polyethylene glycol (PEG) concentration in cryo-experiments, the crystals undergo transformations to the high-ordered form, which was accompanied by shrinkage of the crystals. By the increased use of the cryo-technique, examples of crystal transformations were discovered (Stammers *et al.*, 1994; Cramer & Müller, 1997; Izard *et al.*, 1997; Weiss & Hilgenfeld, 1999).

A holder for free-mounted protein crystals has been described by Kiefersauer *et al.* (1996). The system includes the free-mounting of protein crystals on the pin of a micropipette, humidity control and crystal shape measurements. We present here an improved free-mounting system for protein crystals. Experiments and results for different crystal systems, including CO dehydrogenase (CODH) from the aerobic bacterium *Oligotropha carboxidovorans*, ba_3-cytochrome *c* oxidase from *Thermus thermophilus*, dipeptidyl peptidase IV (DP4) from bovine kidney and periplasmic nitrate reductase (NAP) from *Desulfovibrio desulfuricans*, have demonstrated the use of such a device and method, also in combination with shock-freezing, to improve the crystal quality. The apparatus and experimental results are discussed in this paper.

2. Materials and methods

2.1. The humidity apparatus

A stream of humid air with a defined moisture content is produced (Fig. 1). The dew point T_{dp} of the outcoming mixed gas is measured (MTR 2.12/SA, IL METRONIC Sensortechnik, Ilmenau, Germany). A flexible teflon tube transports the humid air to the crystal holder. The temperature T_{cr} of the crystal holder is controlled. The temperature of the air stream

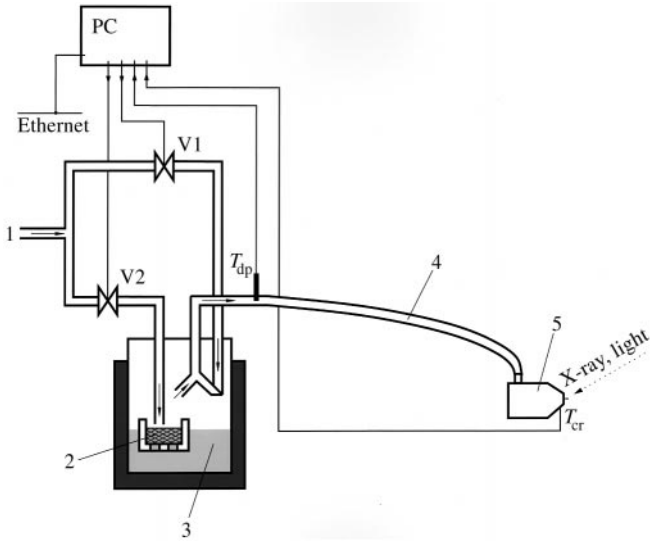

Figure 1
The main functionalities of the humidity apparatus. A line with dry air (1) is split into two; one is saturated with water by blowing onto foam rubber (2). The foam rubber is placed in a perforated plastic vessel in contact with the water reservoir (3). The other line is connected to the outlet of the vessel. The combined humid air stream has a dew point T_{dp}. The flow in both lines (0.8 l min^{-1}) is regulated with the valves V1 and V2. The water reservoir is temperature controlled; water losses are replaced by a pump. The humid air stream is connected to the crystal holder (5) *via* a flexible transport line (4). The tube is heated and isolated to avoid condensation. The temperature of the crystal holder, T_{cr}, is regulated (Industrieregler 48 × 48, RS Components, Mörfelden-Walldorf, Germany) by a thermo-foil and a Pt100 ceramic sensor (Minco, Telemeter Electronic GmbH, Donauwörth, Germany) with an accuracy of ±0.1 K. The crystal is fully accessible for irradiation by X-rays or light.

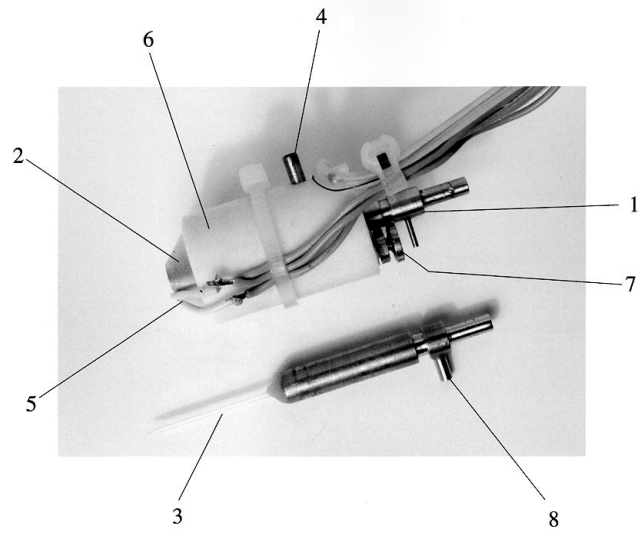

Figure 2
Crystal holder with micropipette. The holding device consists of an insert (1) and a head part (2). The insert holds the micropipette (3), onto which the crystal is sucked by a vacuum line (8). The holding capillary is sealed with glue or wax to the insert. A humid air stream is fed in the head part (4) following two separated channels in the head part which lead into the gas channel. The position of the micropipette tip relative to the outlet of the gas channel is set with the position screw (7). The temperature of the head part is controlled by a thermo-foil and a Pt100 ceramic sensor (5). For better temperature control, the outer head part carrying the thermo-foil is shielded by a teflon cover (6).

is adjusted to T_{cr} by passing through the crystal holder. The relative humidity near the probe follows from the Magnus formula,

$$\text{r.h.} = \exp\left\{a_w\, b_w \left[\frac{T_{dp} - T_{cr}}{(b_w + T_{dp})(b_w + T_{cr})}\right]\right\} \times 100\%,$$

with the constants $a_w = 17.5043$ and $b_w = 241.2$ K. Typically, the temperature T_{cr} is chosen to be at least 1–2 K above the ambient temperature. By the use of two separated valves, V1 and V2, a humidity range of 0–100% can be adjusted within ±0.3%. A personal computer controls the valves V1 and V2 *via* step motors. Arbitrary humidity time protocols, such as humidity jumps or defined humidity gradients, can be realised. The host computer is connected to a computer network. External processing and evaluation of humidity experiments is therefore possible.

2.2. The crystal holder

The crystal holder is shown in Fig. 2. A very compact construction allows the probe to be mounted in a controlled environment with minimal restriction of the X-ray measurements. The head part is freely rotatable relative to the insert, without axial movement. This is an important feature of the holding device as it prevents damage of leads or supplies when the insert is rotated during the measurement. A heating element and a temperature sensor are integrated into the head part. The humid air streaming through the head part is adjusted to the temperature of the head part independently of the ambient temperature. The holding capillary is a patch-clamp pipette with a tip diameter in the micrometre range. The tip is broken off and ground to create a flat mounting surface for the protein crystal. The diameter of the tip of the micropipette should match the size of the protein crystal. The entire crystal holder is fixed on a goniometer head.

A second type of holding device was constructed that employs a loop holder, as used for cryo-transfer of samples, instead of a micropipette (Fig. 3). The loop holder can be removed from the head part and stored in liquid nitrogen. The head part is freely rotatable relative to the insert, as in the device above.

2.3. Mounting the crystal

Initially, the humidity should be adjusted to correspond to the growth conditions of the crystals. An optical method to determine the correct humidity is described by Kiefersauer *et al.* (1996). This method is particularly suitable for high-salt conditions, whereas for PEG or 2-methyl-2,4-pentanediol (MPD) solutions, the method is of limited use. In most cases the 'native' humidity is in the range 92–95% r.h.

Mounting of a protein crystal with the micropipette is illustrated in Fig. 4. A loop is used to remove the crystal from the storage solution. The crystal is sucked up by the capillary using

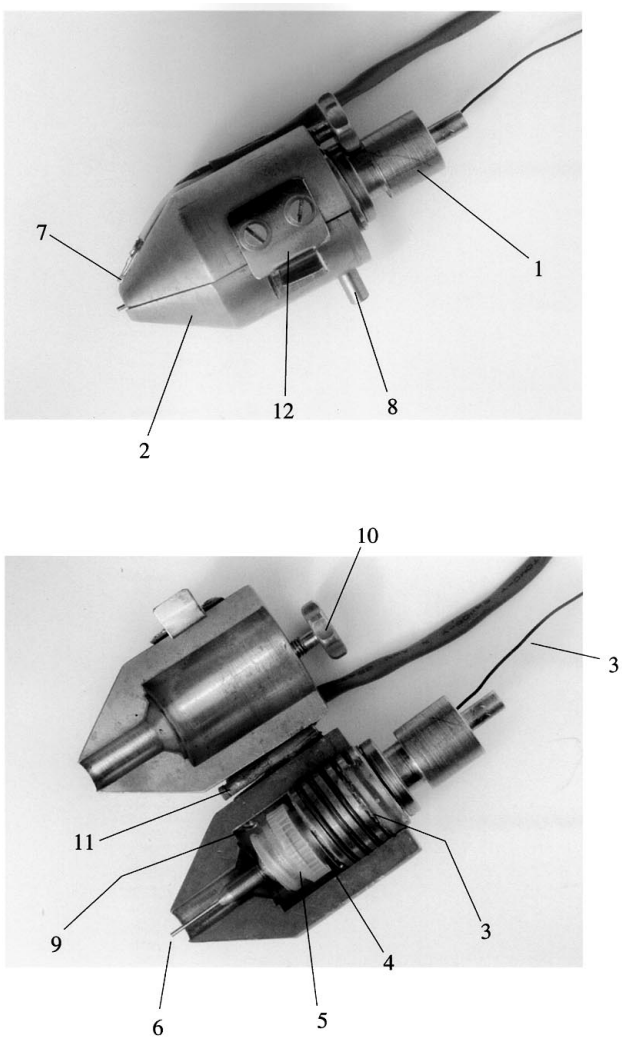

Figure 3
Crystal holder with loop. The construction is similar to that of the crystal holder with a micropipette. A needle-bearing (SKF, Schweinfurt, Germany) and the heating element (3) (Thermocoax, Phillips Elektronikindustrie, Hamburg, Germany) are fixed on the insert (1). The loop holder comprises a magnetic base part (4), a support part (5) and the loop (6). The temperature of the head part (2) is monitored with a temperature sensor (7). The gas entering the head part *via* the side duct (8) is guided through branches to the corresponding opening (9). The position of the loop relative to the outlet of the gas channel is set with the position screw (10). The head part is divided into two shells, which are connected by a joint (11). On the opposite side, the shells are gripped with a spring (12).

a low pressure (0.1 bar). At all steps of the mounting procedure, the crystal is prevented from drying by a stream of humid air.

Using the loop technique, the protein crystal has to be kept free of surrounding crystallization solution to avoid delayed equilibration. Perfluoropolyether (PFPE) was used as the carrier solution. PFPE shields the crystal from the surrounding atmosphere. The oil is put onto the surface of the growth solution. Because of its high density, PFPE sinks to the bottom of the storage chamber together with the crystal. After removing the remaining mother liquor, the crystal can be picked up with the loop. The loop is then positioned on the

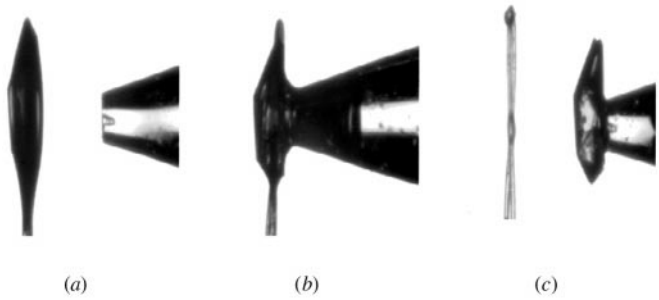

Figure 4
Mounting the crystal on the micropipette. The droplet containing the crystal is placed near the pin of the micropipette in the humid air stream (*a*). Position markers, preadjusted by a micromanipulator, define the correct position relative to the micropipette. In the next step, the pin is gently contacted with the crystal surface whereas some mother liquor is sucked into the micropipette by capillary forces (*b*). At this stage, the vacuum is switched on and the crystal is sucked onto the tip. The loop holder is removed; the crystal is free from solution (*c*). These operations are performed under a stereo microscope (M3Z, Leica, Switzerland).

magnetic base of the opened crystal holder. Finally the shells are closed and held by a spring. To allow faster equilibration of the crystal with the surrounding humid gas stream, the oil coating around the crystal should be as thin as possible.

2.4. Shock-freezing of the sample

A combination with shock-freezing is readily practicable. During the humidity experiment, a mechanical shutter in front of the cryo-nozzle shields the crystal from the cold nitrogen gas stream. For flash-cooling, the crystal is positioned in front of the shutter, the humidity flow is switched off and the shutter is opened. The crystal can then be transferred into liquid nitrogen for storage.

2.5. Optical analysis of the crystal

Mounting the crystal on the tip of the micropipette allows the detection of shadow projections *via* a video system. With the method of back projection, the crystal shape and crystal volume can be easily calculated (Kiefersauer *et al.*, 1996; Izumi *et al.*, 1996). The response of the crystal lattice towards humidity changes can be monitored over time by analysing the crystal extension.

3. Results and discussion

3.1. Optical analysis of tetragonal lysozyme crystals

Tetragonal lysozyme crystals are favourable samples to study hydration/dehydration phenomena because large crystals of good quality can be grown in a few days. Crystals were produced as described in the literature (Steinrauf, 1959).

The appropriate humidity of 89% for the free-mounting system was determined by the loop method. Then the crystal was mounted on the tip of the micropipette as described above. A series of projections were recorded, dependent on the crystal orientation φ with the relative humidity as a

parameter. The humidity was reduced to 76% in steps of 0.5%. Before recording the projections, the crystal was equilibrated at the new humidity value. The change in extension of the projections perpendicular to the rotation axis relative to the initial humidity was analysed. The result is depicted in Fig. 5. Shrinkage of the crystal occurred, which was at first isotropic, then anisotropic. The minima and maxima of shrinkage are separated by 90°. The characteristic curves can be derived by the assumption of a shrinkage without changing the angles between crystal planes, which is confirmed by a comparison of the recorded shadow projections (Kiefersauer, 1998). In the crystallographic *c*-axis direction, the crystal extension shows a hysteresis (Fig. 6). Interestingly, the crystal order was correlated with distinct points of the hysteresis curve. Dehydration and rehydration were fully reversible. The anisotropic shrinkage of the crystal can be explained by the direction-dependent lattice forces in tetragonal lysozyme crystals, as described by Nadarajah & Pusey (1996).

3.2. CODH

The CO dehydrogenase from the aerobic bacterium *Oligotropha carboxidovorans* crystallizes in an orthorhombic space group, $P2_12_12_1$, with cell dimensions a = 129.1, b = 142.4 and c = 167.8 Å. Crystals measured at room temperature diffracted to 3.0 Å and showed a rapid decay in diffraction quality on a conventional rotating-anode generator. To gain higher resolution and phase information through multi-wavelength anomalous diffraction (MAD) measurements, it was necessary to measure CODH crystals with synchrotron radiation. As conventional cryo-protectants (various alcohols like MPD, 2-propanol, 2*R*,3*R*-butanediol and sugars) destroyed the crystalline order, shock-freezing with oil-coated crystals was tried. The crystals were left in 5 µl of the crystallization buffer and coated with 9:2 paraffin/*n*-heptane. After the remaining crystallization buffer was removed with small paper strips, the crystals were picked up and shock-frozen. Crystals treated this way could be frozen, diffracted to 2.0 Å and showed reduced cell constants, but also a highly increased mosaicity, of more than 1°, and overlapping reflections. Freezing without destruction of the crystalline order was finally possible by crystallizing the protein under altered conditions with 15% of glycerol. The crystals showed the same space group and cell dimensions as before. Before measurement, the glycerol concentration was gradually increased to 25%, allowing flash-cooling in the nitrogen gas stream, with good diffraction quality to 2.8 Å on a conventional rotating anode. The crystal structure of the air-oxidized form has been determined at 2.2 Å resolution with synchrotron radiation and MAD measurements of the natural iron clusters in the molecule (Dobbek *et al.*, 1999).

3.2.1. Crystal transformation. As crystal shrinkage went hand in hand with an increase in resolution of diffraction, crystals were tested on the free-mounting system, allowing controlled dehydration of the sample. In a first experiment, the crystal was mounted on the pin of the micropipette and the humidity was adjusted so that the crystal was stable without changing its extension (native state). The crystal diffracted to 3.0 Å with cell dimensions as above. In the next step, the humidity was reduced by 6% to 89% (1% min^{-1}); the crystal then diffracted to 2.2 Å with unchanged mosaicity. The cell constants were reduced to a = 123.4, b = 133.8 and c = 167.1 Å. A further reduction of the humidity led to an increase in mosaicity.

In a second experiment, a different humidity protocol was used. Starting from the native state, the humidity was reduced

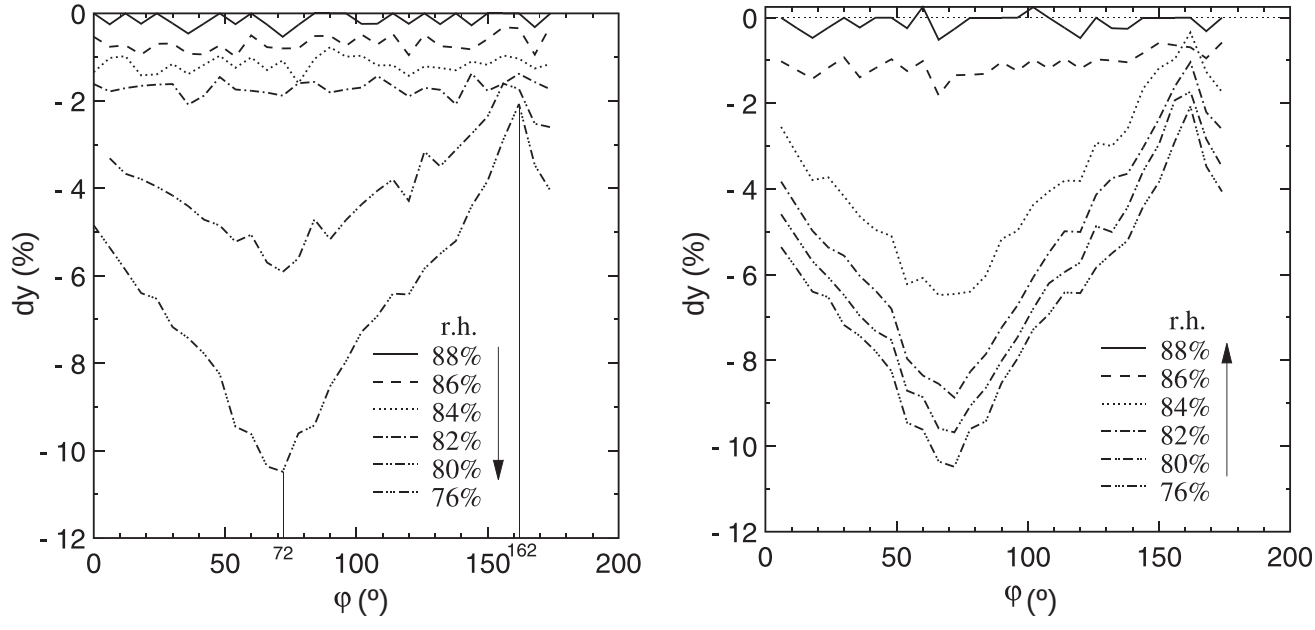

Figure 5
Tetragonal lysozyme transformation. Plotted is the extension of the projections relative to the native state (dy) dependent on the crystal orientation φ with a resolution of 6° for different fixed humidities. The humidity changes are in opposite directions in the right- and left-hand graphs. The equilibration time for each humidity step was 7 min.

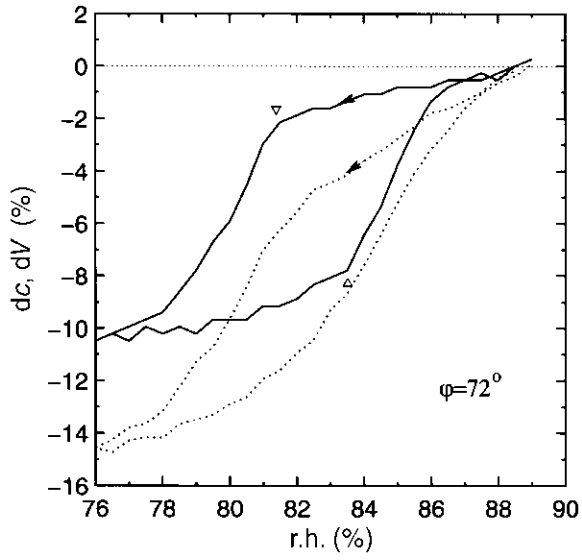

Figure 6
Tetragonal lysozyme transformation. The crystal orientation is held fixed at $\varphi = 72^\circ$ (see Fig. 5). Plotted is the relative change of the crystal dimension in the direction of the crystallographic *c* axis (solid) and of the volume (dotted) dependent on the humidity. At position $\triangledown$, the crystal order disappeared, whereas at position $\triangle$, the crystal order appeared again.

by 11% to 84% with a humidity gradient of 1% min^{-1}. A large improvement of the crystal diffracting power was accompanied with a strong increase of the mosaicity [Fig. 7 (1–1) to (1–5)]. The unit cell shrank by 17% in volume with $a = 119$, $b = 132$ and $c = 162$ Å. A further reduction of the humidity by 3% led to destruction of the crystal order. Surprisingly, a humidity jump to 90% restored the crystal, resulting in 0.2° mosaicity with reflections of 1.8 Å resolution visible. Even though the humidity was increased by 9%, the cell dimensions remained unchanged.

The same protocol for crystal transformation could be applied to oil-coated crystals mounted on a cryo-loop. The success of the transformation depended strongly on the speed of dehydration, with a transformation time below 1 h. Shock-freezing of the crystals resulted in a further reduction of the cell constants to $a = 119.3$, $b = 132.4$ and $c = 160.6$ Å. The frozen crystals showed an additional increase in diffraction power when compared to the transformed crystal, but also a slight increase of the mosaicity from 0.2° to 0.35–0.4°.

3.2.2. Special gases. To determine the crystal structure of the reduced form, anaerobic conditions were necessary. In order to avoid oxidation, Ar or N_2 of high purity was used as carrier gas. The crystals were mounted on the pin of the micropipette and, by changing the humidity, transformation to the high-order crystal form was achieved, as described before. The crystals were reduced by mixing H_2 or CO in the main stream during humidity regulation. The reduction could be followed under the microscope by observing a colour change.

From previous experiments it was clear that methanol or formaldehyde inhibits the activity of CODH. Soaking the crystals with low concentrations of the inhibitors destroyed the crystals. Alternatively, we supplied them *via* the gas phase by generating a saturated gas stream and mixing it with the main stream. This was performed at a position in the gas supply shortly before the point of the dew-point measurement, so that humidity control was ensured. The methanol-saturated gas stream was regulated by a valve.

3.3. Oxidase

Crystals from the membrane protein ba_3-cytochrome *c* oxidase, from *Thermus thermophilus*, were studied using both transformation methods, based either on oil or the humidity-regulated air stream. These crystals belong to the space group $P4_32_12$, are 0.2 to 2 mm in size and contain in their native state 65% solvent. The native crystals showed a great variation in their cell constants ($a = b = 112$–116, $c = 174$–190 Å) and diffraction power. When mounted in standard glass capillaries, they even changed their cell constants, by up to 10 Å for the long cell edge, within hours of X-ray data collection, without clear correlation with environmental conditions. It is obvious that a stabilization of the cell constants was necessary for the collection of useful data sets by either cryocrystallography or by clear control of the environment of the crystal.

Initial experiments devoted to establish a useful cryo-protocol were based on aqueous buffers including a wide variety of cryo-protectants, freezing protocols and precipitant composition. Several conditions could be identified under which the crystals diffracted well after transfer to the cryo-buffer and ice formation was prevented upon freezing. However, the crystalline lattice was always destroyed in the freezing step, resulting in a very low diffraction power and extensive mosaic spread. The first successful freezing protocol could be established by using paraffin oil instead of an aqueous buffer as cryo-protectant and freezing after the oil-enclosed crystal was left for a sufficient amount of time in the cryo-loop. Dehydration occurred by evaporation of solvent through the oil layer. During dehydration, the change of the crystal lattice and crystal order was followed *via* the diffraction images [Fig. 7 (2–1) to (2–2)]. The crystal was frozen after the quality of the images had reached its optimum, thereby preserving the system in this optimal state [Fig. 7 (2–3)]. Analysis of the resulting diffraction images yielded cell constants that were significantly below the range observed for the native crystals; furthermore, the diffraction power had increased. The experiment repeated at the synchrotron allowed structure determination to 2.4 Å resolution using MAD phasing (Soulimane *et al.*, 2000).

This initial indication of crystal transformation effects was then studied more systematically with the free-mounting system. Each crystal was mounted on the pin of the micropipette at a humidity value corresponding to the native state of the crystal. With the free-mounting system, the crystal was stable and it was possible to measure a complete data set of the native crystal form (*c* axis = 178 Å) and to solve the structure by molecular replacement with the MAD structure as the reference system. From humidity values recorded over time, the humidity stability was determined to ±0.5% with a

measuring period of 10 s, and to ±0.1–0.2% by averaging over 10 min. The refined cell constants of the data set calculated by *MOSFLM* (Leslie, 1999) showed a fluctuation of less than 0.7 Å, while they had varied by 10 Å in a capillary.

To follow the crystal transformation, first a slow humidity gradient (1% 30 min^{-1}) was chosen to prevent high mosaicity of the transformed crystals. Lowering the humidity by 2% relative to the native state resulted in the best ordered crystals with a corresponding *c* axis of 172 Å [Fig. 7 (2–4) to (2–5)]. A further slow reduction in humidity distorted irreversibly the crystal lattice. The correlation between relative humidity, resolution and cell dimension was studied by humidity gradients (Fig. 8). This shows that better ordered crystal states occur at well defined humidities and are reached best by steep humidity gradients. The steepest humidity gradient was 1% $(4\ min)^{-1}$. After dehydration of the crystal to about 67% [1% $(4\ min)^{-1}$] and rehydration to the native state, the crystal diffracted as well as before.

Freezing the crystals in a cold nitrogen stream was reproducible only at the crystal stage c = 160 Å. The native state could not be frozen. Freezing of the crystal stage of the first optimum (c = 172 Å) resulted in disruption of the crystal order. Preparing crystals for synchrotron measurements, crystals were mounted in a cryo-loop using PFPE oil. Transformation was then induced by controlled dehydration, which was slowed down remarkably by the oil layer. To obtain higher humidity gradients necessary for better diffraction optima, an initial humidity jump to a low humidity level was investigated (98% to 74% r.h.). Shortly before reaching the cell dimension of the favoured crystal stage, the humidity was regulated back to the corresponding humidity value known from previous experiments. Again, only the crystal stage with c = 160 Å could be frozen without any loss of crystal quality. The diffracting power was about 0.3 Å less than that of the first optimum, but clearly better compared with the native state.

3.4. DP4

Crystals of DP4 (dipeptidyl peptidase IV), from bovine kidney preparations, showed high sensitivity towards manual handling, changes in buffer concentrations and temperature. Even opening of the crystallization vials would cause cracking of the crystals. Crystal mounting in glass capillaries and measurement of diffraction data at room temperature suffered from these problems. The best resolution that could be obtained at room temperature on a rotating anode was approximately 4 Å and the patterns showed rapid decay of diffraction over time. To increase the stability of the crystals and to gain resolution using synchrotron radiation, several cryo-protectant buffers were tested with regard to their influence on crystal stability and freezability. However, all tested solutions either cracked the crystals upon addition or the morphologically unchanged crystals were found not to diffract any more. Addition of 2*R*,3*R*-butanediol to the cryo-protectant buffers resulted in diffraction patterns below 7 Å.

Since the crystals were grown in a solution of low PEG concentration, we also tried to transform the crystals slowly into cryo-protectant concentrations within the mother liquor by simply drying the drop containing the crystal for up to 1 h at room temperature, thus concentrating the PEG. Crystals treated in this way diffracted to about 4–5 Å resolution; however, they also showed an ice ring. In order to define reproducible environmental conditions, we decided to use the free-mounting system for defined dehydration of the DP4 crystals.

3.4.1. Crystal transformation. Crystals mounted on the micropipette were stable at 93.5% r.h. After dehydration, initial experiments already showed an improvement of the crystal order from 5 Å resolution to 3.7 Å. But the diffraction pattern of the transformed crystals showed split reflections. This could be induced by mechanical forces during the mounting procedure, by which, especially, the plate-like crystals were affected.

Mounting the crystals under PFPE oil was the most gentle way of preparing the crystals for X-ray measurements. For this purpose, the oil was placed on the surface of the growth solution by piercing the cover tape of the CrysChem plates (Charles Supper Co., USA) with a syringe needle. The crystals were then mounted in the loop as described before. Such mounted crystals showed very weak diffraction images with reflections of 5 Å resolution at best [Fig. 7 (3–1)]. Dehydration of the crystals from 93.5 to 83% with a gradient of 0.5% $(20\ s)^{-1}$ transformed the crystals to the high-order crystal form, with visible reflections of 2.8 Å [Fig. 7 (3–2)]. The diffraction image showed a clear pattern with low mosaicity. Freezing of the sample in the cold nitrogen stream was successful. The diffraction image showed unchanged quality with respect to resolution and mosaicity [Fig. 7 (3–3)]. The crystals were then stored in liquid nitrogen for measurement with synchrotron radiation.

3.5. NAP

Periplasmic nitrate reductase (NAP), from the sulfate-reducing bacterium *Desulfovibrio desulfuricans*, crystallizes in space group $P3_121$ with cell dimensions $a = b$ = 106.1, c = 134.8 Å. Crystals were obtained using PEG 8K as precipitant, as described previously (Dias, Bursakov *et al.*, 1999). These crystals grow overnight at room temperature to 0.2 × 0.2 × 0.2 mm, and to a maximum size of 0.8 × 0.3 × 0.2 mm in 3 to 5 days. After a few days in the crystallization drop, the NAP crystals undergo a degradation, revealed by the total absence of diffraction spots without any optical indication. Only very fresh crystals were used for diffraction experiments. The best crystals usually diffracted up to 3 Å, using a conventional rotating-anode generator, but the crystal quality varied strongly from crystal to crystal. The NAP crystals were extremely sensitive to radiation. After an exposure time of 30 min at room temperature, the crystals mounted in a capillary did not diffract any more. In order to collect complete data sets and to solve the structure by MAD methods using synchrotron radiation and a single crystal, it was essential to take advantage of cryo-techniques. The crystals were soaked for 5 min with a cryo-protectant solution containing 25% glycerol and 8% PEG 8K before flash-freezing occurred. The

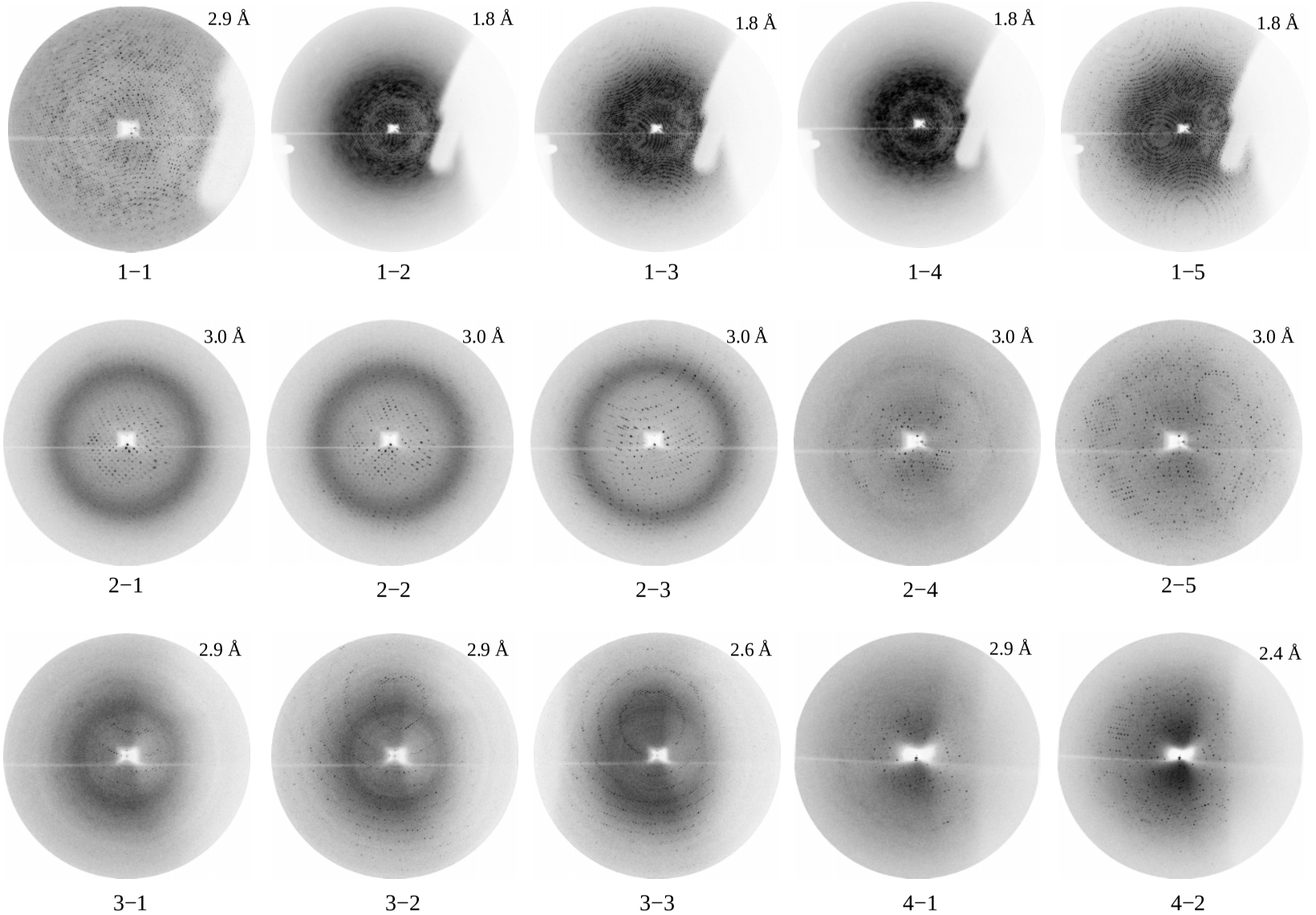

Figure 7
Crystal transformation. The corresponding resolution at the edge of the image is indicated. CODH transformation: (1–1) to (1–5), showing the response of the crystal order during variation of humidity recorded by diffraction images. (1–1) The adjusted humidity was 96% (native state). (1–2) The humidity was reduced to 93%. (1–3) The humidity was further reduced to 84%. (1–4) The humidity was reduced to 81%. (1–5) A humidity jump to 90% was applied. Oxidase transformation: (2–1) to (2–5). The crystal was mounted in a loop with oil as carrier. The diffraction images (2–1) and (2–2) were exposed for 3 min. Then the crystal was frozen, (2–3). The crystal was mounted on the pin of a micropipette. (2–4) The humidity was adjusted to 99%; the cell constants were $a = b =$ 117.5 and $c = 192.6$ Å. The humidity was then reduced by 2%, (2–5). The new cell constants were $a = b = 114.9$ and $c = 172.9$ Å. DP4 transformation: (3–1) to (3–3). The crystal was mounted in a loop with oil as carrier. (3–1) The adjusted humidity was 93.5%. The humidity was then reduced to 83% with a gradient of 0.5% $(20\ s)^{-1}$, (3–2). (3–3) The crystal was then shock-frozen. The exposure time for all images was 3 min. NAP transformation: (4–1) to (4–2). The crystal was mounted on the pin of a micropipette. (4–1) The humidity was adjusted to 97%. After dehydration to 95%, the humidity was then increased to 99.5%, (4–2). Reflections beyond 2.6 Å resolution are visible. The exposure time for both images was 3 min.

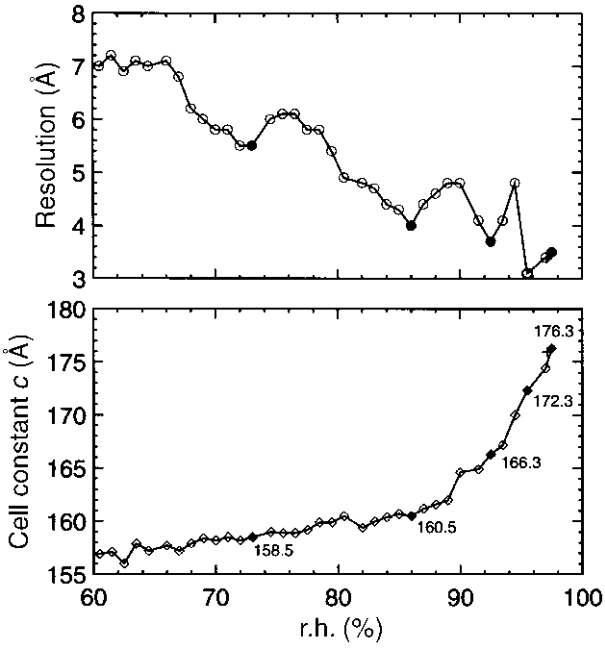

Figure 8
Oxidase transformation. The change of diffraction power and cell constant c with humidity is depicted. The humidity was varied by a gradient from 97.5% down to 30% with a rate of 1% $(4\,\text{min})^{-1}$. Diffraction images were recorded and analysed with *MOSFLM*, resulting in the indicated values for the resolution limit and cell constant. Several preferred crystal forms are clearly visible, which correspond to the resolution optima. These preferred states as well as the native crystal are marked with filled symbols and the cell constants are given. After reaching 30% relative humidity (r.h.), the humidity was again increased to 97.0%, the crystal equilibrated overnight, and two more diffraction images were taken. The crystal returned to its original state (+ symbol).

crystal structure of NAP in the air-oxidized form was determined to 1.9 Å (Dias, Than *et al.*, 1999).

3.5.1. Crystal transformation. Crystals of NAP were mounted on the micropipette of the crystal holder at an adjusted humidity of 97.0% [Fig. 7 (4–1)]. A dehydration of the crystal by only 2% r.h. was accompanied by a continuous loss of crystalline order. The diffraction pattern showed only few reflections near the image centre, *i.e.* to a maximum resolution of around 5 Å. Rehydration of the crystal near 100% r.h. regenerated the crystal order [Fig. 7 (4–2)]. Despite the short exposure time, a well defined diffraction pattern with intense reflections was visible. A series of diffraction images indicated the improved stability of the crystal in the X-ray beam compared with capillary-mounted samples. The crystals diffracted up to a higher resolution of 2.4 Å in a reversible manner, depending on the hydration level of the crystal. NAP crystals provide a rare example of crystal order improvement by hydration relative to the native state.

4. Conclusions

The reported experiments with five different protein crystals show that hydration and dehydration are in most cases reversible processes, passing through defined polymorphic states associated with changes in shape, unit-cell dimensions and crystalline order. The relative humidity *and* its rate of change were found to be important parameters which have to be explored. The technique and apparatus described offer a quite general method to explore the effect of variation of humidity on crystals and in many cases to improve the quality of macromolecular crystals very significantly.

We would like to thank Hans-Ulrich Demuth and Probiodrug/Halle for supplying pure bovine DP4 and Marianne Braun for preparing the DP4 crystals. We are grateful to Saulius Grazulis for the help in programming the humidity regulation and image processing under Linux. The financial support by the EU-Biotech project BIO4-CT98-0418, by PRAXIS XXI/BD/13530/97 and by the Human Frontier Science Program (RG-203/98) is kindly acknowledged. Further information on the use of the apparatus can be obtained from R. Kiefersauer and Proteros (e-mail: info@proteros.de).

References

Bragg, W. L. & Perutz, M. F. (1952). *Acta Cryst.* **5**, 323–328.
Cramer, P. & Müller, C. W. (1997). *FEBS Lett.* **405**, 373–377.
Dias, J. M., Bursakov, S., Carneiro, C., Moura, J. J., Moura, I. & Romão, M. J. (1999). *Acta Cryst.* D**55**, 877–879.
Dias, J. M., Than, M. E., Humm, A., Huber, R., Bourenkov, G. P., Bartunik, H. D., Bursakov, S., Calvete, J., Caldeira, J., Carneiro, C., Moura, J. J., Moura, I. & Romão, M. J. (1999). *Structure*, **7**, 65–79.
Dobbek, H., Gremer, L., Meyer, O. & Huber, R. (1999). *Proc. Natl Acad. Sci.* **96**, 8884–8889.
Huxley, H. E. & Kendrew, J. C. (1953). *Acta Cryst.* **6**, 76–80.
Izard, T., Sarfaty, S., Westphal, A., Kok, A. D. & Hol, W. G. (1997). *Protein Sci.* **6**, 913–915.
Izumi, T., Tsuruta, K., Fujitsuka, A., Kuchiji, H. & Kurihama, T. (1996). *J. Appl. Cryst.* **29**, 435–437.
Kiefersauer, R. (1998). *Kapillaren-freies Montieren von Proteinkristallen unter kontrollierter Feuchte. Vorrichtung und methodische Nutzung.* Dissertation, Technische Universität München.
Kiefersauer, R., Stetefeld, J., Gomis-Rüth, F. X., Romão, M. J., Lottspeich, F. & Huber, R. (1996). *J. Appl. Cryst.* **29**, 311–317.
Leslie, A. G. W. (1999). *Acta Cryst.* D**55**, 1696–1702.
McPherson, A., Malkin, A. J. & Kuznetsov, Y. G. (1995). *Structure*, **3**, 759–768.
Nadarajah, A. & Pusey, M. L. (1996). *Acta Cryst.* D**52**, 983–996.
Schick, B. & Jurnak, F. (1994). *Acta Cryst.* D**50**, 563–568.
Soulimane, T., Buse, G., Bourenkov, G. P., Bartunik, H. D., Huber, R. & Than, M. E. (2000). *EMBO J.* **19**, 1766–1776.
Stammers, D. K., Somers, D. O., Ross, C. K., Kirby, I., Ray, P. H., Wilson, J. E., Norman, M., Ren, J. S., Esnouf, R. M., Garman, E. F., Jones, E. Y. & Stuart, D. I. (1994). *J. Mol. Biol.* **242**, 586–588.
Steinrauf, L. K. (1959). *Acta Cryst.* **12**, 77–79.
Weiss, M. S. & Hilgenfeld, R. (1999). *Acta Cryst.* D**55**, 1858–1862.